Australian Geological and Remote Sensing Services

32 Wheelwright Road
Lesmurdie,
WA 6076
AUSTRALIA

Ph:- +618 9291 7929
Fax:- +618 9291 8566
Email:- bob@agarss.com.au

ASTER Alteration Mineral Mapping; Northwest Tasmania; Australia

Resource Finance & Investments Limited

Bob Agar

PROJECT DETAILS

Project Title:	ASTER Alteration Mineral Mapping; Northwest Tasmania, Australia.
Project Status:	Strictly confidential
Client:	Resource Finance & Investments Limited
Contact:	Mark Derriman
Contact Details:	Resource Finance & Investments Limited Exploration Manager Ground Floor 43 Ventnor Ave West Perth 6005 Tel. (+1) 303-973-8585 Fax (+1) 303-973-0715 Email: markd@rfilimited.com
Consultant(s):	Bob Agar
Peer Reviewed By:	N/A
Project Date:	August 2005
Report Completed:	Wednesday May 18th 2005
Additional Comments:	

ASTER Alteration Mineral Mapping; Northwest Tasmania, Australia.

1. Introduction

The Advanced Spaceborne Thermal Emission and Reflection Radiometer (ASTER) acquires multi-spectral image data for 15 channels across the visible, near, short wave and thermal infrared wavelengths (table 1).

Subsystem	Band No.	Spectral Range	Spatial Resolution
VNIR	1	0.52-0.60	15m
	2	0.63-0.69	
	3N	0.78-0.86	
	3B	0.78-0.86	
SWIR	4	1.600-1.700	30m
	5	2.145-2.185	
	6	2.185-2.225	
	7	2.235-2.285	
	8	2.295-2.365	
	9	2.360-2.430	
TIR	10	8.125-8.475	90m
	11	8.475-8.825	
	12	8.925-9.275	
	13	10.25-10.95	
	14	10.95-11.65	

Table 1; Band specifications of the ASTER sensor system.

Compared to Landsat Thematic Mapper (TM), which has been widely used as a basic trool in exploration targeting and reconnaissance mapping, the visible and near infrared (VNIR) data have a finer resolution (15 metres), the short wave infrared (SWIR) data at 30m resolution are the same as for Landsat TM bands 5 and 7 but with 6 contiguous channels over the same wavelength range offer far greater spectral resolution, and the thermal infrared (TIR) data with 5 channels and a 90m spatial resolution offer greater spectral and spatial resolution than the single TIR band (band 6 @ 120m) of Landsat TM (Table 1).

The enhanced spatial and spectral resolution of the ASTER instrument over Landsat TM has the potential to overcome conflicts experienced in discriminating specific iron and clay mineralogy by providing sufficient resolution to be able to discriminate individual mineral species (figure 1). Whereas Landsat data cannot discriminate between clay/carbonate alteration minerals with any real confidence, the spectra of common alteration minerals convolved to the ASTER band specifications show that the absorption wavelength associated with the three main styles of alteration, argillic, phyllic and propylitic, moves progressively from 2.165 through 2.209 to 2.36 μm respectively.

Although alunite and pyrophyllite share a common absorption band (2.165μm) their spectra are different. Similarly kaolinite and muscovite both exhibit absorption at the 2.209μm wavelength yet have distinct spectra and the propylitic alteration minerals such as chlorite, epidote and calcite all have a common absorption band at 2.36μm but equally distinct spectra. Thus, individual minerals fall into the same broad absorption bands from which general alteration indices can be calculated but are sufficiently different across the range of the SWIR to be individually mappable in theory (figure 1).

However, it must be remembered that pixels of these dimensions will almost invariably be mixed in terms of their mineralogy and so pure mineral spectra are unlikely. Nevertheless, the spectra for some pixels will be dominated by a single mineral and should show some close resemblance to the spectrum for that particular mineral. However, minerals that occur together produce mixed spectra that can appear very much like another mineral. For example, alunite and kaolinite commonly occur together and their mixed spectra as convolved to ASTER band positions may look like dickite. Thus although a considerable improvement on Landsat TM, ASTER also has the capacity to create significant false mineral zones and care is still required in interpretation of the minerals mapped.

Fourteen of the bands are collected with the sensor looking vertically downward (nadir) but ASTER data also contain an additional VNIR band that is acquired from a rear-looking telescope (Band 3B is Backward-looking, Band 3N is Nadir-looking, table 1). The two band 3s are useful in providing a perspective view that enables the data to be viewed as a stereo pair. The data also contain internal ground control points calculated from the satellite ephemeris that are used to georeference the data and which, in conjunction with the stereo visualisation and parallax effect, enable the creation of digital terrain models (DTMs) and, in rugged terrains, ortho-rectification of the spectral image bands.

Thus, ASTER data represent a considerable improvement upon previous, readily available, broad coverage and low cost spectral remote sensing data in the context of regional mineral exploration studies.

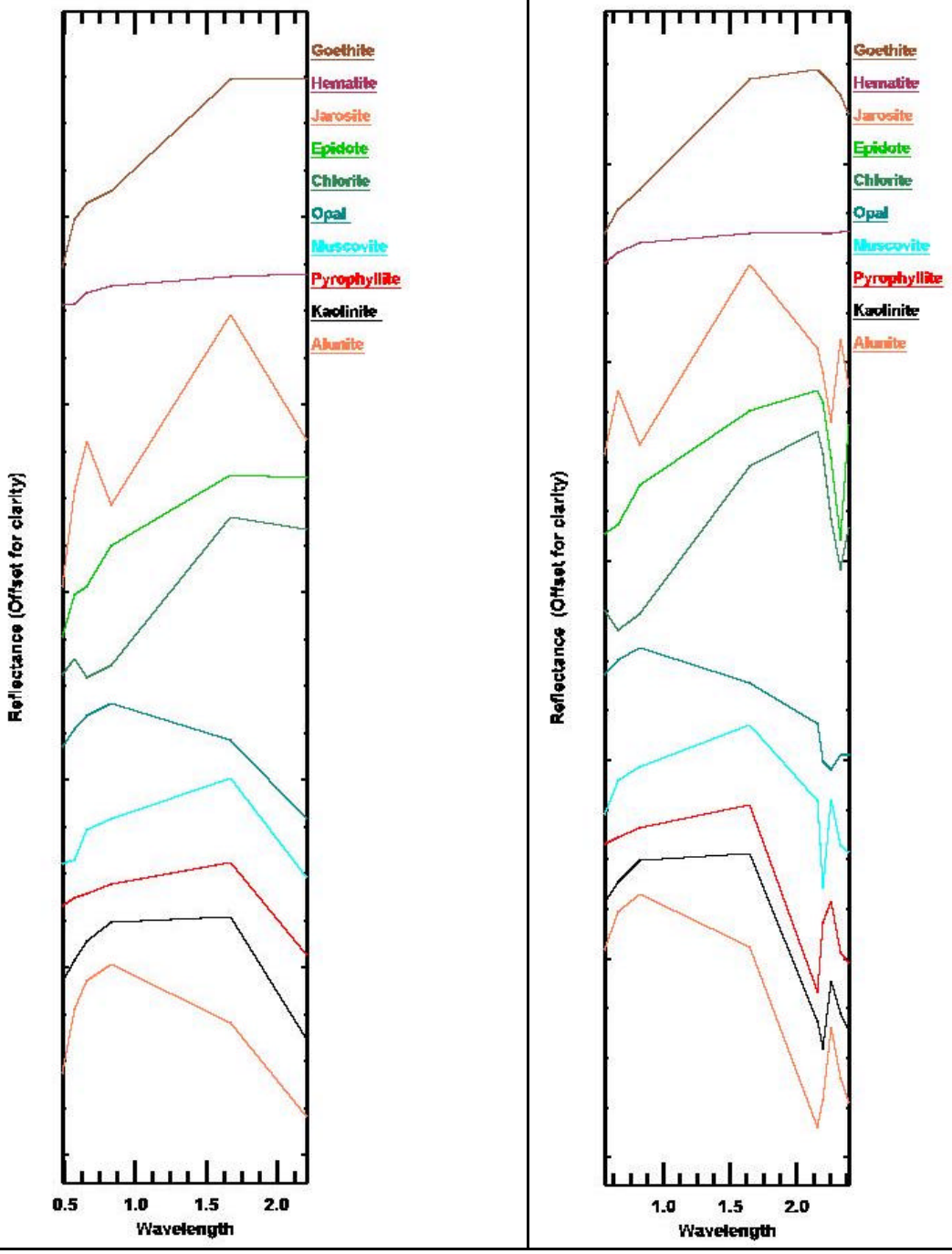

Figure 1; Comparison of Landsat and ASTER spectra of some common alteration minerals.

However, as with all remote sensing work, the efficacy of any data depends to a large extent on the nature of the terrain being imaged and the signal:noise characteristics of the data. As a general rule, hyper-arid terrains such as the Atacama Desert of Northern Chile afford the best climate and geologic exposure for mineral exploration applications. These data have very high signal:noise characteristics due to the clean dry atmospheric conditions combined with high soil and rock exposure. Elsewhere, other desert terrains are also ideal for remote sensing purposes but as one moves into semi-arid and progressively more humid climes, the amount of vegetation in the region and the atmospheric humidity both increase. Furthermore, away from the tropics towards higher latitudes, the sun elevation at the time of acquisition is lower and hence signal strength also falls. The sun elevation and atmospheric humidity issues combine to reduce the data quality and the presence of vegetation, including lichen and mosses, acts to modify mineral spectra to the extent that the spectra of normally distinct minerals are sufficiently obscured or modified as to be lost within the general noise and vegetation spectra.

2. Processing and Interpreting ASTER data.

2.1 Processing ASTER Data

ASTER data were sourced to cover the study area as defined by tenements held in northwestern Tasmania (figure 2). Unfortunately, cloud free or cloud limited (less than 20%) data were not available for the entire area and those data that were available contained significant cloud (figure 2).

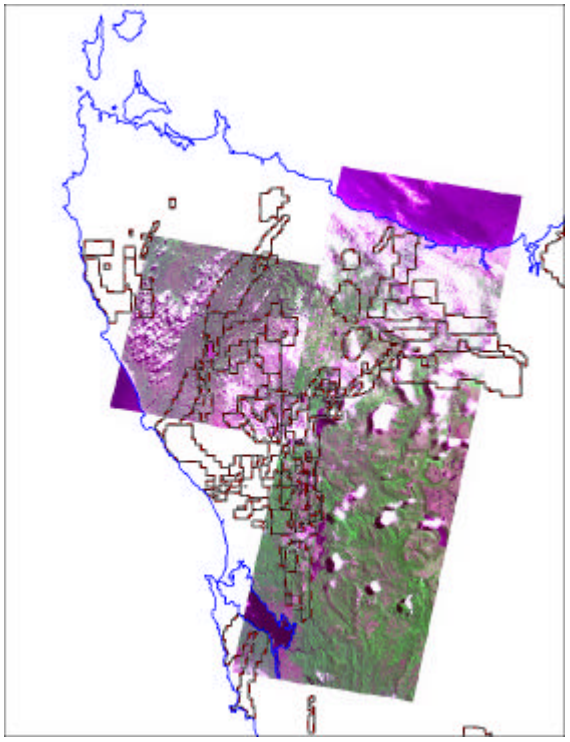

Figure 2; Simulated true colour images of ASTER scenes acquired in northwest Tasmania for the purpose of this study relative ot the outline of tenements held. Note the significant amount of cloud cover in each of the three scenes but the relatively clear ground over much of the area under claim.

The following four ASTER level 1B, radiance at sensor, scenes from 2 separate acquisition dates were purchased:-

Image Strips and Scene IDs			
Path	**Row**	**View**	**Acquisition Date**
91	246	2	23rd August, 2001
92	245	7	3rd February 2001
92	246	7	3rd February 2001
92	247	7	3rd February 2001

The L1B scenes are pre-processed to radiance at the sensor and were used to create a Digital Elevation Model (DEM) using the AsterDTM ENVI add on software of Sulsoft (Brazil) and this same DEM was in turn used to ortho-correct each of the image bands. Scenes that were acquired on the same day as part of a single data capture were then mosaicked together and treated as a single image strip for subsequent processing.

Radiance at the sensor data comprises the reflectance from the ground plus artefacts such as energy that is backscattered by particles such as dust or water vapour in the atmosphere and electronic noise. In ASTER data, the digital number recorded at the sensor is also affected by an energy "overspill" or "cross-talk" problem between detectors. Energy from ASTER band 4 "leaks" and affects the digital number being recorded in other bands, most notably bands 5 and 9 (figure 3). Both of these effects need to be corrected for before converting the data to reflectance.

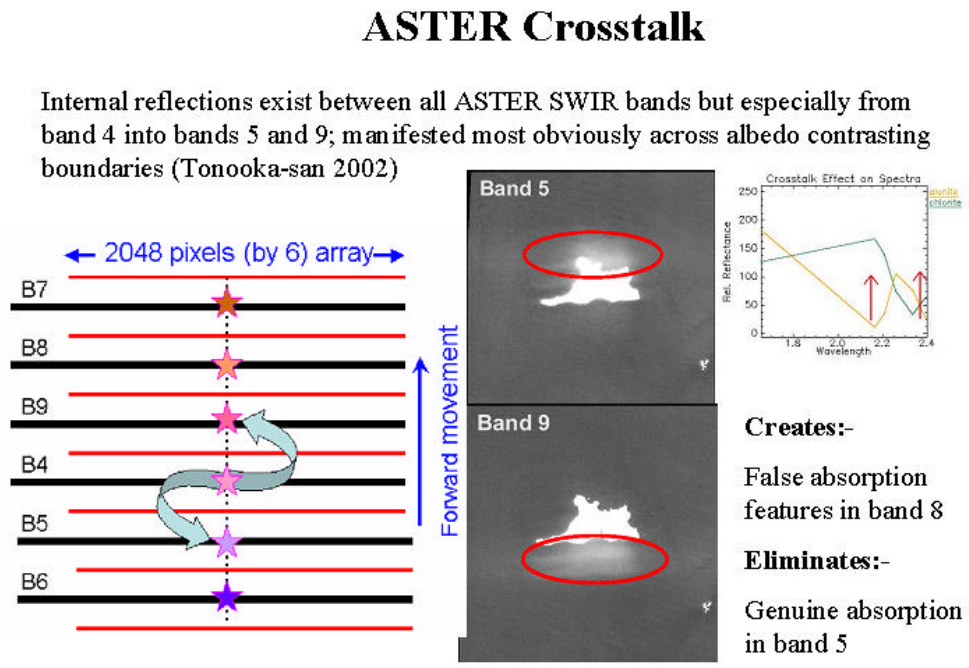

Figure 3; Schematic representation of the "crosstalk" problem in the ASTER SWIR module

The atmospheric backscatter component is greatest at shorter wavelengths and most pronounced for ASTER data in band 1, diminishing exponentially to be insignificant in the SWIR bands. The effect is very significant however in the VNIR bands where the spectra for the iron oxide minerals are separated from vegetation and each other by the relationship between bands 1, 2 and 3 where, for the iron minerals, band 1 is consistently low relative to bands 2 and 3 and a critical slope change occurs at band 2 which signifies vegetation. If the backscatter is not corrected, band 1 will be artificially high and result in fewer iron minerals being mapped. Bodies of water typically have a very flat spectrum in the VNIR and the response over known water bodies was used here to generate a spectrum representing the atmospheric backscatter that was subsequently removed from every pixel. As a check, pixels over obvious vegetation were checked in the corrected data to confirm that their spectra were showing band 1 (natural green) higher than band 2 (natural red).

Similarly, the "cross-talk" problem in the SWIR bands was removed using a spectral unmixing technique in RASTUS software to identify the "cross-talk" spectrum and remove it from each pixel in turn. Unless removed, "cross-talk" will record artificially high values in bands 5 and 9, diminishing apparent absorption in band 5 thereby reducing the potential for mapping alunite and pyrophyllite; increase the apparent absorption in band 6 thereby increasing the amount of kaolinite, and white micas (e.g. sericite, illite, phengite) mapped and increase the apparent absorption in band 8 thereby mapping chlorite, epidote and calcite more widely than it should (figure 1).

Once these corrections to the radiance data had been carried out, the data were then converted to reflectance using the "log residual" normalisation technique (Green & Craig, 1985) in RASTUS software. From these reflectance data, areas of cloud were masked out and then mineral indices were prepared and analysed separately for each constituent scene or data capture series. Indices were prepared for the suite of minerals using the methodology as listed in table 2.

The minerals selected are typical of those found in a variety of mineralised hydrothermal and metasomatic (skarn-type) systems and the reference spectra are taken from the USGS spectral library available in ENVI software and convolved to the ASTER band positions. The suffix number of each reference spectrum is that from the USGS reference library.

Two muscovite indices were created in an attempt to map any variability in muscovite mineralogy from high AlOH variants (referred hereinafter as sericite) to low-AlOH (more MgOH, FeOH bearing and referred to hereinafter as phengite). The wavelength position of the maximum absorption in muscovite minerals is known to be controlled by the mineral chemistry and to range from 2194nm for high AlOH up to 2219nm for the low AlOH (figure 4a). Although the ASTER data cannot map such a wavelength shift in the absorption band, the ASTER spectra do show a variation in the shape of the absorption band at 2209nm (Figure 4b).

As a further means of detecting phyllic alteration and to provide a simple index for the probable wavelength position of maximum absorption (i.e. position in the sericite – phengite continuum), a phyllic index was created using simple band ratios to select only pixels that had a phyllic absorption feature at band 6 and the ratio 7/5 was used to provide a proxy numerical index of the wavelength position, higher values to the high-

AlOH/low wavelength end of the continuum such that high-AlOH minerals would have values >1 and low AlOH <1 in this index (figure 4 and table 2).

Mineral or Style	Index processing routine
FeOx	Mask of ratios 2/1, 3/2, and 3/1 within known ranges for goethite, hematite and jarosite applied to PC3 of PC123
Goethite	Mask of ratios 2/1, 3/2, within known ranges for goethite; applied to VNIR MF result for goethite 1.
Jarosite vnir	Mask of ratios 2/1, 3/2, within known ranges for jarosite; applied to VNIR MF result for jarosite 6.
Haematite	Mask of the FeOx index with jarosite and goethite pixels removed.
Advanced Argillic	Mask of ratios 4/5>1; 5/6<1; 7/6>1; 7/5>1; 7/8>1; 9/8<1, 5/8<1, 5/9<1 applied to ratio 7/5.
Argillic	Mask of ratios 4/5>1; 5/6>1; 7/6>1; 7/5>1; 7/8>1; 9/8<1, applied to ratio 7/6
Phyllic	Mask of ratios 4/5>1; 5/6>1; 7/6>1; 7/8>1; 9/8<1, 6/8<1, 6/9<1 applied to ratio 7/6 for intensity and ratio 7/5 for AlOH composition
AlOH	Mask of ratios 4/5>1; 7/6>1, 7/8>1; applied to ratio 7/6
Propylitic	Mask of ratios 4/5<1, 5/6>1, 7/6<1, 7/5<1,7/8>1,9/8>1, 5/8>1, 6/9<1 applied to ratio 5/8.
Carbonate	Mask of ratios 4/5>1, 5/6>1, 7/6<1, 7/5<1, 9/8>1, 6/9<1 applied to ratio 5/8.
SiO2	Mask of band ratios 12/13<1; 12/11<1; 13/11>1; 11/10>1 applied to TIR MF result for silica
Alunite	Mask of ratios 4/5>1; 5/6<1; 7/6>1; 7/5>1; 7/8>1; 9/8<1, 5/8<1, 5/9<1 applied to SFF result for Alunite 1
Pyrophyllite	Mask of ratios 4/5>1; 5/6<1; 7/6>1; 7/5>1; 7/8>1; 9/8<1, 5/8<1, 5/9<1 applied to SFF result for Pyrophyllite 3
Dickite	Mask of ratios 4/5>1; 5/6>0.99<1.01; 7/6>1; 7/5>1; 7/8>1; 9/8<1, 5/8<1, 5/9<1 applied to SFF result for Dickite 1
Kaolinite	Mask of ratios 4/5>1; 5/6>1; 7/6>1; 7/5>1; 7/8>1; 9/8<1, 6/8<1, 6/9<1 applied to SFF result for Kaolinite 7
Sericite (High-AlOH phyllic)	Mask of ratios 4/5>1; 5/6>1; 7/6>1; 7/5>1; 7/8>1; 9/8>1, 6/8<1, 6/9<1 applied to SFF result for Muscovite 4
Phengite (Low-AlOH phyllic)	Mask of ratios 4/5>1; 5/6>1; 7/6>1; 7/5<1; 7/8>1; 9/8>1, 6/8<1, 6/9<1 applied to SFF result for Muscovite 3
Jarosite swir	Mask of ratios 4/5>1; 5/6>1; 7/6<1; 7/5<1; 7/8<1; 9/8<1, 6/9>1 applied to SFF result for Jarosite 2
Opal	Mask of ratios 4/5>1; 5/6>1; 7/6<1; 7/5<1; 7/8<1; 9/8<1, 6/9<1 applied to SFF result for Opal 2
Dolomite	Mask of ratios 4/5>1; 5/6>1; 7/6<1; 7/5<1; 7/8<1; 9/8>1, 6/9>1 applied to SFF result for Dolomite 1
Calcite	Mask of ratios 4/5>1, 5/6>1, 7/6<1, 7/5<1,7/8>1,9/8>1, 5/8>1, 6/9<1 applied to SFF result for SFF result for Calcite 3
Chlorite	Mask of ratios 4/5<1, 5/6>1, 7/6<1, 7/5<1,7/8>1,9/8>1, 5/8>1, 6/9<1 applied to SFF result for SFF result for Chlorite 3
Epidote	Mask of ratios 4/5<1, 5/6>1, 7/6<1, 7/5<1,7/8>1,9/8>1, 5/8>1, 6/9<1 applied to SFF result for SFF result for Epidote 3
Garnet	Mask of ratios 12/13>1; 14/13>1; 12/14>1; 12/11>1; 13/11<1, 14/11<1; 14/10<1 applied to TIR MF result for garnet
CO3	Mask of ratios 14/13<1; 12/13<1, 12/11>1, 13/11>1, 11/10>1, 12/14>1, 14/11<1, 14/10<1 applied to MF result for TIR CO3.

Table 2; Alteration minerals mapped and their respective processing routines and algorithms.

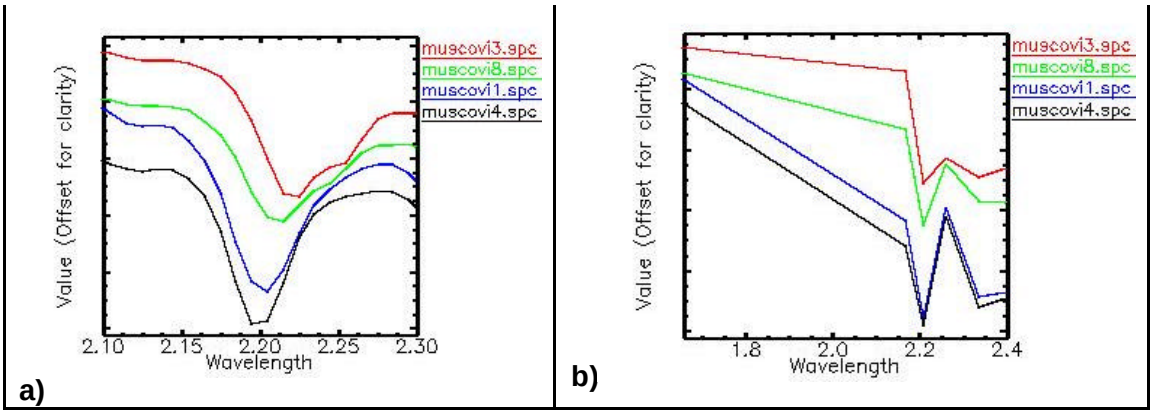

Figure 4; a) Standard USGS reference spectra for high AlOH (muscovi4), moderately high AlOH (muscovi1), relatively low AlOH (muscovi8) and low AlOH (moscovi3) showing the progressive shift of the absorption band position to longer wavelengths and b) the same spectra convolved to the ASTER band configuration showing the variation in the shape of the 2209nm absorption band for the same minerals.

The spectral feature fit (SFF) routine in ENVI software uses a least-squares fit approach to measure the closeness of fit between an image or pixel spectrum with a reference spectrum (Clark et al., 1990) and is directly proportional to the depth of the spectral feature and mineral abundance. This method was used to create indices for alteration minerals with spectral features in the SWIR because the method is direct although it is reputedly more sensitive to illumination, albedo and aspect effects than other methods.

The SFF routine is used in conjunction with masks generated using arguments based upon band ratio properties to define only those pixels with spectra approximating the reference to reduce noise and false positives (table 2).

A matched filter (MF) routine also in ENVI is a rapid partial unmixing process that focuses on and maximises values where there is a match and suppresses the response for the composite unknown background. It works well and is used for the VNIR, where the spectra are simple (3 bands), and in the TIR but gives inconsistent results and is thus not used for the SWIR minerals. However, in both the VNIR and the TIR, the MF routine is again used used in close conjunction with band ratios to eliminate possible false positives. The band ratio masking algorithms for the VNIR and SWIR are derived from USGS reference mineral spectra and those in the TIR derived from mineral emission spectra taken from the John Hopkins Spectral Library in ENVI.

An alternative approach, the Spectral Angle Mapper (SAM) method developed in ENVI software from the work of Kruse and others (1993), measures the angular difference between the image spectrum and the reference spectrum but produces an inverted image in which the lowest values represent the closest match. In this author's experience, the method has given inconsistent results for many minerals and is used only in instances where the albedo and aspect effects preclude use of SFF.

With the exception of the FeOx, goethite, jarosite-vnir, haematite, AlOH, advanced argillic, argillic, phyllic, propylitic, carbonate, SiO2, garnet and CO3 indices, which were generated using band ratios values as constraints (table 2), thresholds were determined for each mineral index by first filtering pixels according to band ratio constraints listed in table 2 before visually comparing the remaining pixel spectra against a reference spectrum using a simple density slice routine to highlight the different index levels. Where the top pixel values for the index of any mineral did not exhibit characteristic or diagnostic spectral features of that mineral, the mineral was omitted from the final output.

Where a threshold could be determined, only those pixels with index values greater than the threshold were preserved and ultimately used to create the full regional mosaic index. This image was saved as the final index for that mineral and a region of interest created from the index marking those pixels assigned to that mineral in a specific colour. The index was then filtered using a combination of closing and median filters to consolidate clustered pixels into zones and eliminate outliers or noise. These pixels were also defined as a colour coded smoothed region of interest and saved together for final output visualisation. The filtered index image was finally exported as both a vector file delineating the smoothed occurrence boundaries for each mineral and as a pseudo-colour raster image draped over albedo to show variation in intensity for each mineral.

The regions of interest, both individual pixel and filtered, were individually displayed on a greyscale albedo background so as to provide an overview of the distribution of the various alteration minerals. Unfortunately, in ENVI software, later created regions of interest overprint the earlier ones where they overlap. This is not an issue for the alteration minerals in the SWIR because the way in which the regions are generated means they would not overlap or only minimally overlap. However, the iron oxide and silica regions, being created in the VNIR and TIR data respectively can and do overlap the other minerals. Thus care should be taken in interpreting the region of interest output image.

Alteration style indices produced for FeOx (ferruginisation) SiO2 (silicification), advanced argillic, argillic, phyllic, propylitic and carbonate were also saved as both pixel regions of interest mapping all possible pixels with appropriate characteristics and as filtered regions of interest. The output for all alteration style indices were smoothed and filtered as for the individual mineral indices and both region of interest images, intensity images and vector outputs prepared.

Some indices map very extensively. Garnet for example maps more widely than would be anticipated due to its spectral similarity to mafic rocks. For this reason, the garnet index is further thresholded at the 97% probability level so as to map only the top 3% of the possible pixels. Haematite also maps very widely because it lies spectrally between goethite and jarosite end members. For this reason, the Matched Filter index for haematite is unreliable and the FeOx index is used instead. Haematite is therefore more of an indication of iron enrichment that cannot be attributed to either goethite or jarosite. Because it also maps extensively, it is also thresholded at the 97% probability level.

The outline boundary vectors for each mineral and alteration style were imported into MapInfo and can be visualised either individually or collectively. The advantage here is that where overlaps occur, the ornament allows that overlap to be noted and some idea

of the total mineral assemblage can be generated. These vector files can be attributed in such a way as to permit interactive interrogation of the ASTER output data with other data sets in a GIS.

Other output includes standard ER Mapper files for 2-3-1 (rgb); 6-3-1 (rgb); 5-6-8 (rgb), albedo, a RGB combination of FeOx, AlOH, and SiO2 (FAS) indices, as well as pseudo-colour images showing the variation in intensity for each mineral identified. The 2-3-1 (rgb) image is a simulated true colour image whereas the 6-3-1 RGB image is an ASTER equivalent of the standard Landsat 7-4-1 (rgb) image product and can be interpreted similarly. The 5-6-8 (rgb) image however shows alteration styles of advanced argillic in blue tones, argillic and phyllic in pink-red tones and propylitic in yellow-green tones. The FAS (rgb) image shows iron rich areas in red, hydrothermally altered areas in yellow and silicified zones in blue. Combined iron-clay anomalism is yellow in colour, iron-silica magenta, clay-silica cyan, and all three combined is white. Furthermore, a Digital Elevation Model (DEM) was produced for the granule and from this a pseudocolour shaded relief image created and exported into MapInfo. All output images have been compressed using the ER Mapper ECW compression and subsequently imported into MapInfo for display with the vector files as a single MapInfo workspace. In addition to the MapInfo output files, the vectors have also been saved as ESRI Shape files to allow import into Arc-View or Arc-Info GIS software.

In addition to a regional mosaic compiled from the results for all three image strips, workspaces and output for each if the individual strips were also compiled. From these, it was apparent that a number of mineral indices were also mapping vegetation and potentially obscuring mineral alteration zones. To overcome this issue, a Normalised Difference Vegetation Index (NDVI) was calculated for each of the image strips and values greater than 0 used to create a mask to eliminate those pixels with a significant amount of vegetation. The individual mineral indices were then masked and new output generated without the conflicting spurious vegetation derived "mineral" zones. The indices in the individual image strip output were left with the vegetation unmasked.

2.2 Interpreting ASTER Data

The quality and reliability of the resultant mineral distribution maps can only be judged against accurate field observations and mapping. However, some observations with regard to the output products are relevant.

As noted above, pixels of these dimensions will almost invariably be mixed in terms of their contents and so pure mineral spectra are unlikely. Where a mineral has been mapped, the mineral mapping in this study assumes that the pixel spectrum represents a single mineral. However, minerals occurring together produce mixed spectra that can appear very much like another mineral. For example, an equal mix of kaolinite and alunite appears spectrally like dickite in the ASTER band configuration (figure 5).

The nature in which certain alteration minerals occur should always be taken into consideration. For example, in hydrothermal settings, pyrophyllite and dickite typically occur in narrow veins and are unlikely to spectrally dominate a wide zone of 30m ASTER pixels. Thus, indications of their presence might represent a mixture of other more common minerals. Additionally, although the reference spectra used for the mineral mapping are those of hydrothermal alteration minerals, some are very similar to

a host of other minerals that may also be present. For example, the phyllic minerals mapped as sericite or high-AlOH phyllic and those mapped as phengite or low-AlOH phyllic are in a spectral continuum that includes muscovites, illites, and montmorillonites, all of which are indistinguishable at this spectral resolution (figure 6). Similarly, although chlorite and epidote are used for the propylitic minerals, it is important to remember that the propylitic mineral spectra will also likely capture occurrences of high-MgOH clays derived from mafic rocks. Thus, the minerals mapped should be viewed in their broadest context and not as absolute or perfect examples of those minerals.

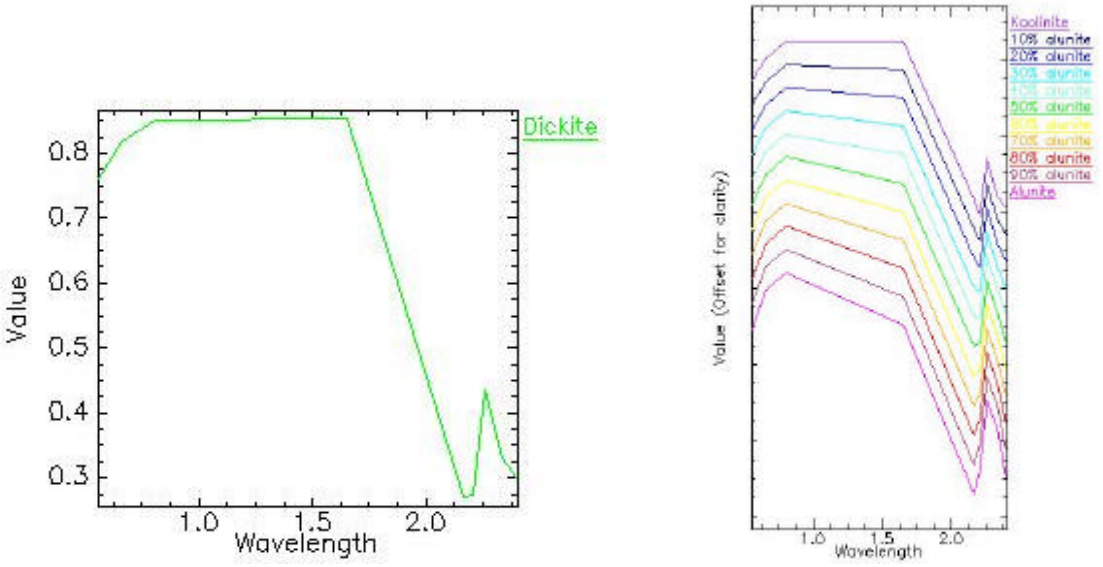

Figure 5; Comparison of dickite spectrum convolved to ASTER band specifications (left) with modelled spectra for various mixtures of kaolinite and alunite. Note the similarity between the dickite and the 50% kaolinite/alunite mixture (green on right).

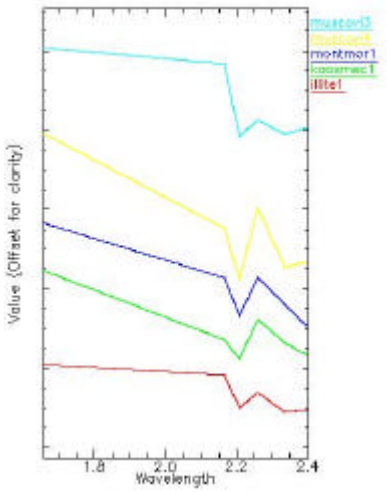

Figure 6; Comparitive plots of ASTER spectra for a range of phyllic minerals showing their overall similarity and hence likelihood for being mapped together

Thus, care must always be taken when interpreting the mineral map and the indicated presence of a particular mineral should be viewed in the context of its spatial coherence, the minerals mapped in close association with it as well as its 3-dimensional distribution. When identifying and characterising alteration zones and systems, associations of the more common alteration minerals are more likely to be indicative of the alteration facies and zones of the rarer minerals viewed more positively if they are indeed narrow and in keeping with their known mode of occurrence. Alteration minerals that map in coherent zones that are 3-dimensionally consistent with known or conceptual alteration systems will usually be more significant than those which occur either in isolation or in rare or obscure associations.

The iron oxide minerals mapped specifically are goethite, haematite and jarosite. The spectral variability of hematite falls within the range of both goethite and jarosite and as such is difficult to map as a specific index. By creating a total FeOx index as applied here, haematite falls within the area not covered by either goethite or jarosite. However, it must be noted also that mixtures of both goethite and jarosite can produce the same spectral shape as haematite and so the mapped distribution of haematite outside the goethite and jarosite end-members should be treated as mixed iron oxides and/or haematite. Goethite and jarosite usually map more discretely and are more likely to be representative of ferruginisation associated with mineralisation. However, the more intense zones of the haematite_97 index might also represent ferruginisation.

The jarosite index generated using the SWIR does not match that of jarosite using the VNIR bands. This is not unusual in so much as the spectral absorption feature for jarosite in the SWIR is often subdued in the presence of opaline silica. A combination of the two minerals is quite common in reality with the jarosite frequently occurring only on fracture surfaces and not being exposed to the sensor across the full area of the pixel. Combinations of jarosite and opaline silica are also frequently indicated within ASTER imagery. This may be a real association but care must be exercised in interpreting such associations because the spectral absorption features for both minerals are at the same wavelength and each mineral would score highly in the index for the other. Thus, the association may be artificial. Furthermore, where jarosite and/or opaline silica are present with other minerals such as alunite or any of the phyllic minerals, their reflectance and overall strength of spectral features are such that the diagnostic jarosite and opal features are likely to be lost or at best subdued.

Problems with the ASTER data themselves can impact on the way minerals map. The advanced argillic minerals such as alunite and pyrophyllite can be lost due to the energy over-spill or “cross-talk” problem within ASTER band 4 while chlorite, epidote and calcite can map more widely (see above).

Another problem identified in ASTER data concerns instability in the detector for band 4 which can give wide fluctuations in the values for that wavelength, impacting upon the slope between bands 4 and 5 in the spectrum so that absorption is consistently mapped at band 5. Thus, where both pyrophyllite and alunite map more widely than might normally be expected it could be due to this instability problem. Bands 8 and 9 also frequently appear to have anomalously high values and may need to be adjusted by applying a gain factor. When left unadjusted, the abnormally high values in either of these bands can impact greatly on how all minerals map.

Additionally, many minerals share an absorption band with certain vegetation species and care should be taken when interpreting mapped mineral zones that have a greenish colour in the 6-3-1 (rgb) and 2-3-1 (rgb) reference images. Where this problem is widespread, it may be necessary to remove the vegetation by masking or attempting to unmix the vegetation and mineral spectra using any of a number of unmixing algorithms. However, the successful unmixing of vegetation spectra depends upon accurate and usually multiple vegetation species and spectra being identified within the data and, although this routine may work with hyperspectral data is not likely to work with data of ASTER's spectral resolution.

A problem has been identified within many ASTER scenes that is manifested by a band of intermittent bright pixels in processed data such as band ratios and mineral indices but which is not visible in the raw bands (figure 7; Coulter, 2002).

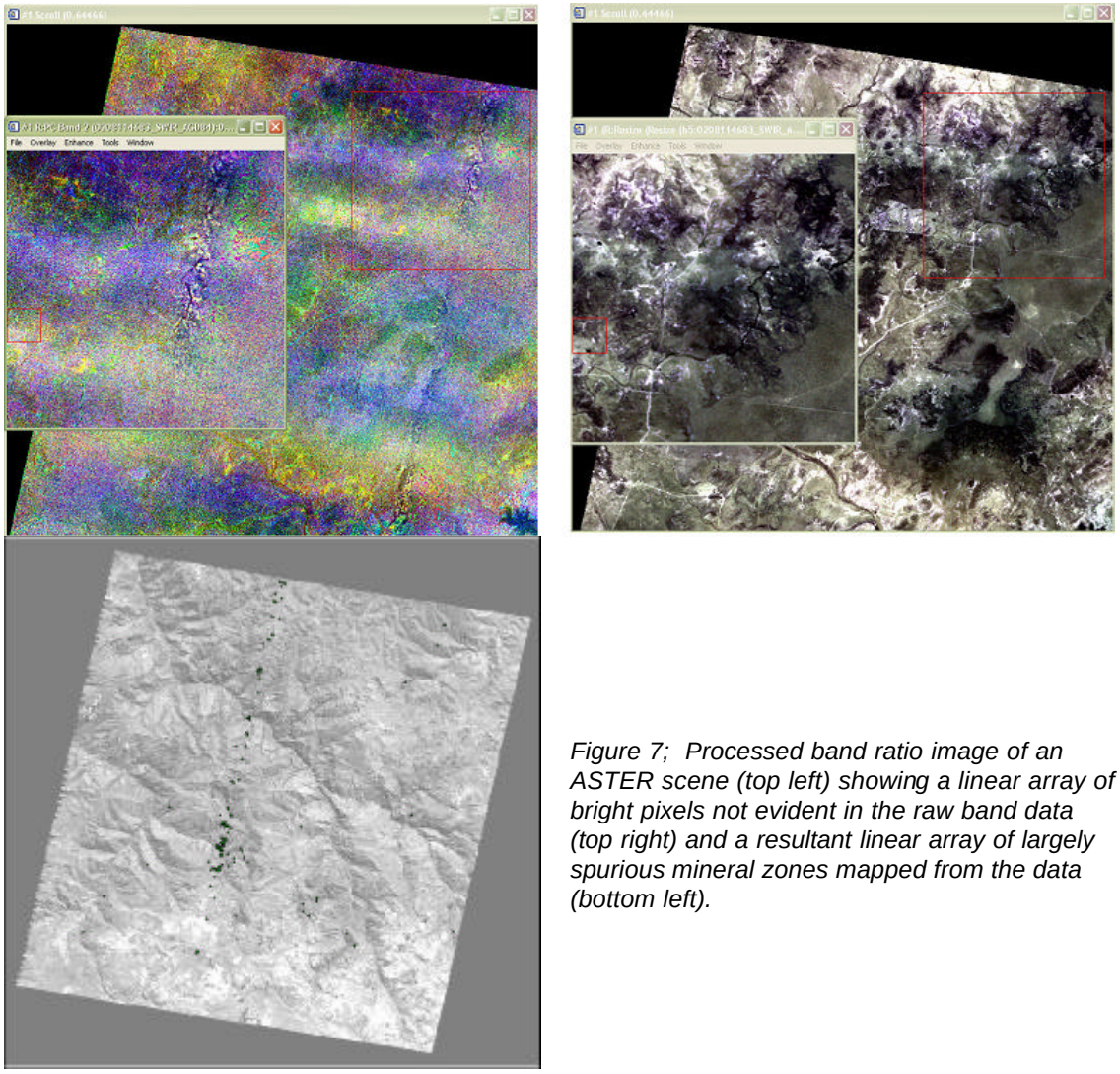

Figure 7; Processed band ratio image of an ASTER scene (top left) showing a linear array of bright pixels not evident in the raw band data (top right) and a resultant linear array of largely spurious mineral zones mapped from the data (bottom left).

The problem has been ascribed to a permanent scratch in the instrument's diffraction grating for the SWIR module causing a distinct change in the signal:noise characteristics

across a certain band of pixels (Watanabe, 2002). There is no correction for this problem. Furthermore, when mosaicking scenes, spurious pixel values can be generated along scene boundaries and produce false anomalies or mineral zones. Thus care should be taken when interpreting alteration that maps in any orbit-parallel array whether within or marginal to an image strip.

All mineral indices, but especially those of the phyllic minerals, can have conflicts with areas of water, cloud, snow and ice but these can easily be recognised when interpreting the data by checking the output against the 6-3-1 (rgb) and 2-3-1 (rgb) reference images. Both very commonly map to areas of deep shadow in scenes with high albedo contrast due to the "cross-talk" effect and care should be exercised in interpreting such zones.

The advanced argillic, argillic and phyllic minerals commonly map extensively along the northern shores of water bodies. The cause of this phenomenon is not clear but may be a similar effect to the harmonic "cross-talk" effects noted above or may be due to other factors such as an increase in humidity local to large water bodies. In any event, the phenomenon should be noted and caution taken in drawing any significance from such mapped mineral zones.

The propylitic and calc-silicate minerals are typically dark and relatively low in reflectance by comparison with other minerals being mapped. Frequently they map to areas of shadow and caution should be exercised in interpreting any areas identified as being of these minerals that are in significant shadow. They are also often in conflict with vegetation and once again care should be exercised in interpreting areas indicated as being propylitic or calc-silicate minerals that are also green in the 6-3-1 (rgb) or 2-3-1 (rgb) reference images.

Garnet is mapped using the TIR bands and usually maps much more widely than would be expected, probably due to the presence of mafic within the area covered by the scene. Mafic and carbonate rocks have a similar thermal emission spectrum and hence skarn alteration should be interpreted only where garnet is indicated in conjunction with carbonate and calc-silicate minerals.

3. ASTER Data Analysis and Field Follow-Up

Without access or reference to existing published geological data or field verification, analysis of these ASTER data at this stage can only be general and in terms of degrees of confidence in the output based upon the geological coherence of the mapped minerals and alteration styles with respect to one another and to other features such as topography and possible structural features such as lineaments and fractures.

In these data, the advanced argillic, argillic and phyllic minerals noticeably map along the northern shores of water bodies and almost all of the minerals map widely in vegetated areas. Whereas the vegetation effect has been masked out of the final mosaic products, the coastal effect cannot be removed and should be taken into account when reviewing the data.

Once the vegetation had been largely removed from the data, the different mineral indices map coherently for the most part. However, although clouds had been masked out of the data in pre-processing, many alteration zones still appear to be associated with the fringes of cloud or cloud shadows (figure 8).

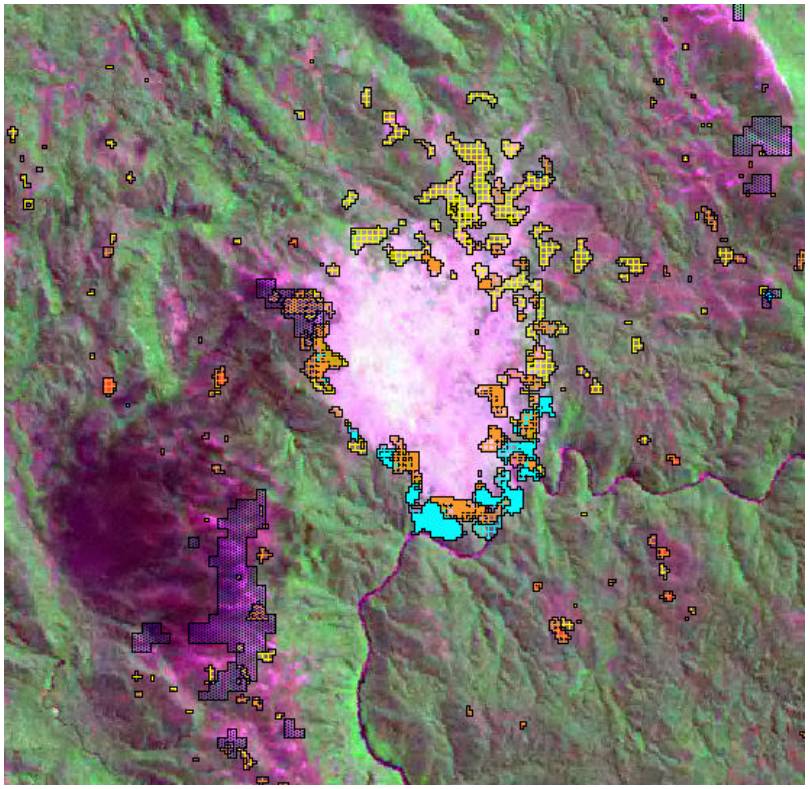

Figure 8; Spurious mineral zones displayed over simulated true colour image showing the edge effects associated with clouds.

In analysing the mapped mineralogy for potential exploration targets, characteristic hydrothermal mineral associations have been sought such as zoned associations of advanced argillic, argillic, phyllic, silicic, carbonate and propylitic alteration with the presence of iron minerals that may represent possible gossan. Alteration targeting has also focussed on the disposition of both individual mineral zones and styles with linear arrays of alteration minerals or styles associated with particular stratigraphy, fractures or lineaments ranked more highly.

The ranking has assigned an arbitrary value of 0.5 for the presence of an alteration style such as argillic plus 0.5 for the indication of a specific mineral of that style such as kaolinite. Added to this would be a value of 0.5 for a clear zonation from high-temperature to low temperature alteration facies plus 0.5 for each lineament direction represented up to a maximum of 3 lineaments, 0.5 for any obvious stratigraphic control, 0.5 for an associated vegetation anomaly. Thus the maximum for any target would be 10. Indications of alteration are listed in table 3. this table and the ranking assigned to each target can and should be revised in the light of additional information on the controls and signatures of known mineralisation in the region. The ranking should also take into account geologic factors such as position in stratigraphy for example and is, at this stage, intended only as a guide to the complexity of alteration styles indicated.

Table 3; Indications of hydrothermal alteration and potential exploration targets.

ID	Easting	Northing	Area	Description	Rank
1	413865	5426532	14.6843	NW oriented silica; adv-argillic (alunite), argillic (kaolinite) zones in phyllic (sericite) located on contact between contrasting propylitic and argillic domains; possibly cloud affected.	5.5
2	406231	5429119	84.9412	Large phyllic (sericite) zone with central adv-argillic (alunite); argillic (kaolinite) and silica zones: also peripheral argillic and propylitic (chlorite). Some cloud.	5
3	399349	5426236	21.4095	Small centres of adv-argillic (alunite, pyrophyllite); and phyllic (sericite) with silica in broader argillic; oriented N-S	4
4	397021	5423378	9.96015	Argillic (kaolinite) with pockets of adv-argillic (alunite) and phyllic (sericite); minor silica; weak N-S orientation	4
5	390296	5425510	62.5053	Cluster of phyllic (sericite); adv-argillic (alunite, pyrophyllite); and argillic zones with silica and minor FeOx (goethite, haematite) fringing cloud and cloud shadow.	4.5
6	352944	5427810	17.2826	Cluster of phyllic (sericite) zones with minor adv-argillic (alunite); argillc; silica and carbonate, fringing cloud.	4
7	329820	5401234	209.808	Large cluster of adv-argillic (alunite); phyllic (sericite); argillic (kaolinite); carbonate; FeOx (jarosite-swir); minor silica; propylitic (chlorite); garnet. No zoning or preferred orientation or shape with zones lying in between clouds and parallel	4.5
8	359379	5410626	15.3293	Mushroom shaped cluster of phyllic (sericite); argillic; adv-argillic; carbonate; FeOx (jarosite-swir); vegetation anomaly; flat side parallels stratigraphy.	5.5
9	376375	5414470	52.1496	Adv-argillic (alunite); argillic; phyllic (sericite); silica; FeOx (jarosite-swir); carbonate (dolomite); possibly some cloud affect;	5.5
10	415330	5408483	47.2119	NW-oriented FeOx (jarosite, goethite, haematite) with silica, argillic and minor adv-argillic (alunite), phyllic (sericite) in contact with propylitic (chlorite)/carbonate (dolomite); also zone parallels edge of cloud shadow	5
11	437480	5385488	11.9864	Zones of adv-argillic (alunite); argillic; phyllic (sericite); and FeOx (jarosite, goethite) oriented N-S	4.5
12	406783	5389126	18.5186	Centre of FeOx (jarosite, goethite); in carbonate with propylitic (chlorite, epidote); and silica plus minor phyllic; oriented NE	5
13	400415	5382010	14.8485	Adv-argillic (alunite, pyrophyllite); argillic (kaolinite, dickite); phyllic (sericite); minor carbonate/propylitic halo; fringing cloud and zonation following aspect to a degree.	3.5
14	391192	5395583	13.2333	Adv-argillic (alunite); argillic (kaolinite); phyllic (sericite); silica; propylitic zones clustered around filmy cloud	4.5

Table 3 continued; Indications of hydrothermal alteration and potential exploration targets.

ID	Easting	Northing	Area	Description	Rank
15	364277	5397020	13.1106	N-S trending cluster of phyllic (sericite); adv-argillic (alunite); argillic zones with silica along contact with carbonate (dolomite) domain - possible cloud affect.	5
16	358968	5391385	98.1566	Relatively bare exposed ground with adv-argillic (alunite); phyllic (sericite); argillic; silica; propylitic (chlorite); carbonate centres - hint of zonation.	5
17	339053	5392082	13.9551	Adv-argillic, argillic, phyllic (sericite); silica; FeOx (jarosite-swir); carbonate zones oriented more or less with stratigraphy apart from one NW trend - possibly following structure. Vegetation anomaly	5.5
18	356285	5380471	49.3057	Clusters of adv-argillic (alunite); argillic; phyllic (sericite); propylitic (chlorite); carbonate; silica; FeOx (jarosite-swir); no coherent zoning, patterns or trends but in structurally interesting zone - ESE/WNW and ENE/WSW linears intersecting.	5
19	422780	5367166	52.3155	Adv-argillic (alunite); argillic; phyllic (sericite); FeOx (jarosite, goethite); carbonate zones	4

All too frequently, alteration zones appear to be spatially associated with the edges of cloud or with water bodies and as such, ranking points were deducted from these unless the mapped mineralogy appeared to trend independently of the cloud or water body. None of the targets ranked higher than a score of 5.5, reflecting the influences of both cloud and vegetation on the processing and in limiting the amount of soil and outcrop contributing to the spectral classification. Nevertheless, these indications of alteration need to be reviewed and evaluated in terms of known geology, geochemistry, geophysics, geomorphology and, in particular structure and known mineralisation in the area. Known mineralisation not highlighted by alteration mapping should be reviewed in terms alteration signatures and scale so that the reason for their absence is understood. This would entail field visits and verification of alteration mineralogy mapped successfully and that not mapped so as to identify any issues of scale, mixtures and/or spectral conflicts between materials present within the region as a whole. Errors of both omission and commission need to be investigated in order to fine tune the database and generate better exploration targets within the region.

One consideration of prime importance is the question of the size and scale of alteration signatures exposed for the known mineralisation. These zones of known alteration can be used to generate ASTER spectra from within these data for use in further classifying and targeting hitherto unknown alteration zones.

Controls on known mineralisation can be used to fine tune the ranking and prioritising of the listed targets as well as to identify others, particularly in the light of structural controls or lithologic parameters such as skarn mineralisation and subtle alteration associated with sediment hosted or low-sulphidation systems for example. Spectra from these areas of known mineralisation can be used to search for similar patterns elsewhere in the study area and ground spectra can also be used to improve the conversion to reflectance of the data set and eliminate any residual “crosstalk” or instrument gain and offset problems.

4. References

Clark, R.N.; Gallagher, A.J. and Swayze, G.A., 1990; *"Material Absorption Band Depth Mapping of Imaging Spectrometer Data Using a Complete Band Shape Least-Squares Fit with Library Reference Spectra."* Proceedings of 3rd Airborne Visible/Infrared Imaging Spectrometer (AVIRIS) Workshop, JPL Publication, 90(54): p. 176 - 186

Coulter, D., 2002; *"ASTER Problems and Resolutions; A Data User's Perspective".* Presented to "ASTER Unveiled," Annual General Meeting of the Geological Remote Sensing Group, Geological Society of London, December 2002.

Green, A.A. and Craig, M.D., 1985; *"Analysis of aircraft spectrometer data with logarithmic residuals."* Proceedings of AIS Workshop, 8-10 April; JPL Publication, 85(41): p. 111 – 119.

Kruse, F.A., Lefkoff, A.B., Boardman, J.B., Heidebrecht, K.B., Shapiro, A.T., Barloon, P.J., and Goertz, A.F.H., 1993; *"The Spectral Image Processing System (SIPS) – Interactive Visualization and Analysis of Imaging Spectrometer Data."* Remote Sensing of Environment, v.44 p.145 –163.

Watanabe, H., 2002; *"Current Status of ASTER, ASTER Ground Data System and its Application."* Presented to "ASTER Unveiled," Annual General Meeting of the Geological Remote Sensing Group, Geological Society of London, December 2002.

Bob Agar, Australian Geological & Remote Sensing Services